research articles Journal of proteome research

Glycomics of Proteoglycan Biosynthesis in Murine Embryonic Stem Cell Differentiation

Alison V. Nairn,[†] Akiko Kinoshita-Toyoda,[‡,§] Hidenao Toyoda,[‡,§] Jin Xie,[||] Kyle Harris,[†] Stephen Dalton,[†] Michael Kulik,[†] J. Michael Pierce,[†] Toshihiko Toida,[‡] Kelley W. Moremen,[†] and Robert J. Linhardt*[,||]

Complex Carbohydrate Research Center and the University of Georgia, 315 Riverbend Road, Athens, Georgia 30602, Graduate School of Pharmaceutical Sciences, Chiba University, 1-33, Yayoi-cho, Inage-ku, 263-8522 Japan, Core Research for Evolutionary Science and Technology (CREST), Japan Science and Technology Agency, 4-1-8 Honcho, Kawaguchi, Saitama 332-0012, Japan, and Departments of Chemistry and Chemical Biology, Chemical and Biological Engineering, and Biology, Rensselaer Polytechnic Institute, Troy, New York 12180

Received July 18, 2007

Glycosaminoglycans (GAGs) play a critical role in binding and activation of growth factors involved in cell signaling critical for developmental biology. The biosynthetic pathways for GAGs have been elucidated over the past decade and now analytical methodology makes it possible to determine GAG composition in as few as 10 million cells. A glycomics approach was used to examine GAG content, composition, and the level of transcripts encoding for GAG biosynthetic enzymes as murine embryonic stem cells (mESCs) differentiate to embryoid bodies (EBs) and to extraembryonic endodermal cells (ExE) to better understand the role of GAGs in stem cell differentiation. Hyaluronan synthesis was enhanced by 13- and 24-fold, most likely due to increased expression of hyaluronan synthase-2. Chondroitin sulfate (CS)/dermatan sulfate (DS) synthesis was enhanced by 4- and 6-fold, and heparan sulfate (HS) synthesis was enhanced by 5- and 8-fold following the transition from mESC to EB and ExE. Transcripts associated with the synthesis of the early precursors were largely unaltered, suggesting other factors account for enhanced GAG synthesis. The composition of both CS/DS and HS also changed upon differentiation. Interestingly, CS type E and highly sulfated HS both increase as mESCs differentiate to EBs and ExE. Differentiation was also accompanied by enhanced 2-sulfation in both CS/DS and HS families. Transcript levels for core proteins generally showed increases or remained constant upon mESC differentiation. Finally, transcripts encoding selected enzymes and isoforms, including GlcNAc-4,6-*O*-sulfotransferase, C5-epimerases, and 3-*O*-sulfotransferases involved in late GAG biosynthesis, were also enriched. These biosynthetic enzymes are particularly important in introducing GAG fine structure, essential for intercellular communication, cell adhesion, and outside-in signaling. Knowing the changes in GAG fine structure should improve our understanding the biological properties of differentiated stem cells.

Keywords: glycomics • embryonic • stem cell • differentiation • glycosaminoglycan • biosynthesis

Introduction

Glycosaminoglycans (GAGs) are linear, anionic polysaccharides found primarily in the extracellular environment of the glycocalyx and extracellular matrix of all animal cells.[1] There are three families of uronic acid containing GAGs, hyaluronan (HA), chondroitin sulfate (CS)/dermatan sulfate (DS), and heparan sulfate (HS) (Figure 1). Over the past 20 years, the GAG biosynthetic pathways have been elucidated. While many of the biosynthetic enzymes have been cloned and expressed, our understanding of both their specificity and how these enzymes are controlled and regulated is not well understood.[2−4] GAG biosynthetic enzymes are often present in multiple isoforms localized in the plasma and Golgi membranes. The expression of these isoforms is often spatially and temporally regulated giving rise to different GAGs in different cell types and at different stages in development.[5,6]

GAGs are important cellular receptors for proteins such as growth factors and are involved in cell signaling, adhesion, growth and differentiation.[1,7] The HS GAG chains of the proteoglycans syndecan and glypican, for example, are responsible for the assembly of the FGF-FGFR signal transduction

* To whom correspondence should be addressed. Center for Biotechnology and Interdisciplinary Studies, Rensselaer Polytechnic Institute, Troy, New York 12180. Tel.: 518-276-3404. Fax: 518-276-3405. E-mail: linhar@rpi.edu.
[†] University of Georgia.
[‡] Chiba University.
[§] Japan Science and Technology Agency.
[||] Rensselaer Polytechnic Institute.

10.1021/pr070446f CCC: $37.00
Published on Web 10/04/2007

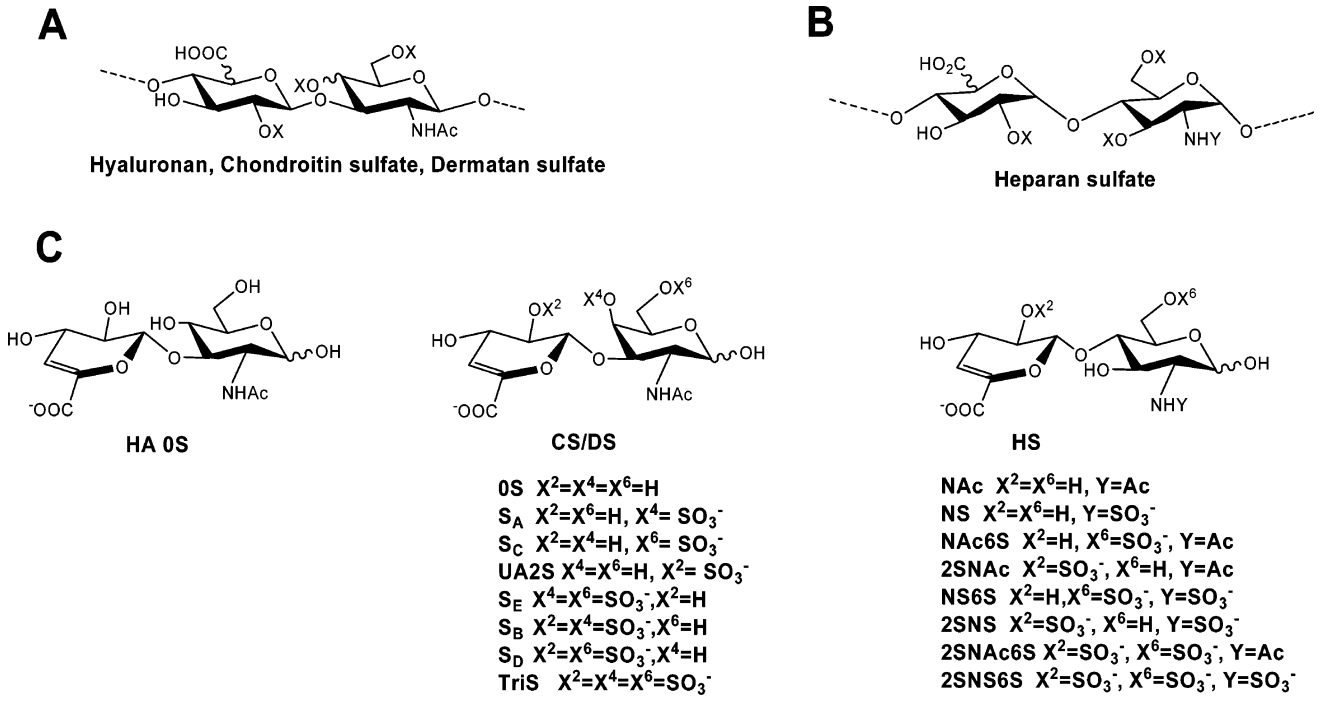

Figure 1. Structure of Glycosaminoglycans. (A) Hyaluronan (uronic acid is GlcA and hexosamine is GlcN and X = H), chondroitin sulfate (uronic acid is GlcA, hexosamine is GalN, more than 2 of the X groups = H and less than one of the X groups = SO_3^-), and dermatan sulfate (uronic acid is IdoA and hexosamine is GalN, more than 2 of the X groups = H and less than one of the X groups = SO_3^-); (B) Heparan sulfate (uronic acid varies from primarily GlcA to primarily IdoA, hexosamine varies from primarily GlcNAc to primarily GlcNS, and X + Y ranges from ~1 to 2.5 SO_3^- groups). (C) Disaccharides afforded on the complete polysaccharide lyase catalyzed depolymerization of GAGs.

complex, an essential component of the early development of diverse organisms.[1,7,8]

Glycomics deals with the study of the structure and function of glycans, glycosphingolipids, glycoproteins, such as proteoglycans, as well as proteins that bind to glycans. An understanding of the glycome will likely explain some mysteries associated with gene regulation via changes in expression and/or post-translational modification.[9] The structural glycomics of the GAG chains of HS proteoglycans from murine tissues have been recently under intensive study by our laboratory.[10] The structure of HS in genetically modified mice has also been examined.[11]

Murine embryonic stem cells (mESCs) are derived directly from the inner cell mass (ICM) of preimplantation embryos[12−14] and have been used extensively as an *in vitro* model in which to study specific aspects of early embryonic development.[15,16] In the presence of IL-6 family members such as leukemia inhibitory factor (LIF), mESCs can be maintained in culture indefinitely in a self-renewing state as a pluripotent stem cell population and retain many of the characteristics of their founder cells in the ICM.[17−20] Throughout extended periods of passaging, mESCs retain their broad differentiation potential *in vitro* and, when introduced back into blastocyst-stage embryos, can contribute to normal development of the entire embryo and to the germ line.[21−23] ESCs have been used extensively to understand the biology of late pre-implantation and early post-implantation development, including events associated with the formation of the three embryonic germ layers,[24,25] but have also generated considerable interest as they are a potential source of cells that can be used to cure degenerative diseases through cell therapy.

In this report, we begin to examine the GAG glycome in mESCs by defining changes in GAG content and structure as pluripotent ESCs differentiate. These data are then complemented by an analysis of the changes in the expression levels of GAG-related transcripts using quantitative RT-PCR (qRT-PCR), an analysis that can detect transcript expression linearly over 7 orders of magnitude. Although a particular transcript level may or may not reflect the expression level of the protein it encodes or the activity of this protein, understanding changes in specific gene transcript levels is an important first step in determining how GAG biosynthesis is regulated during embryonic stem cell differentiation. Overlaying GAG structural and transcript expression changes provides insights into the regulation, synthesis, and expression of GAG structures and lays the foundation for more fully understanding their regulation and possible function during mESC differentiation and embryogenesis. In this report, we begin to examine the GAG glycome in mESCs by defining changes in GAG content and structure as pluripotent ESCs differentiate into either embryoid bodies (EBs), composed of endoderm, ectoderm, and mesoderm, or extraembryonic endodermal cells (ExE) formed through stimulation of monolayers with retinoic acid.

Materials and Methods

Growth and Characterization of mESCs, EBs, and ExE. R1 mESCs[26] were cultured in the absence of feeders on tissue culture grade plasticware precoated with 0.1% gelatin-phosphate buffered saline (PBS), as described previously.[27] mESC culture medium consisted of Dulbecco's Modified Eagle Medium (DMEM, GIBCO BRL) supplemented with 10% fetal calf serum (GIBCO), 1 mM L-glutamine, 0.1 mM 2-mercaptoethanol, 100 U/mL penicillin, 100 U/mL streptomycin, and 1000 U/mL recombinant human LIF (ESGRO) at 37 °C under 10% CO_2. Differentiation of mESCs into embryoid bodies (EBs) was carried out as described previously.[28] mESCs were harvested by trypsinization converting suspensions of single ESCs into aggregates and seeded into 10 cm bacteriological dishes at a

density of 1×10^5 cells/mL, in 10 mL mESC-medium lacking LIF. EBs were harvested daily, the medium was changed every 2 days, and cultures were split one into two at day 4. Differentiation of mESCs into extraembryonic endoderm (ExE) was carried out by treatment with retinoic acid as previously described.[29] Cell populations of mESCs, EBs, and ExE were characterized by flow cytometry using the lineage-specific marker CD9 and by transcript analysis using quantitative RT-PCR. RNA was prepared using Qiagen RNeasy Mini Kits. Chromosomal DNA was removed using RNase-free DNase (Qiagen). cDNA was prepared using the Superscript First Strand Synthesis System (Invitrogen) using 2 μg total RNA. Target mRNAs were assayed using TaqMan Gene Expression Assays (Applied Biosystems), supplemented with Universal PCR Master Mix (Applied Biosystems). PCR reactions were performed on an Applied Biosystems ABI 7700 Sequence Detector. Paired samples for each cell type were used for both structural and qRT-PCR analysis.

Recovery and Disaccharide Compositional Analysis of GAGs. GAGs were prepared from approximately 20 mg of lyophilized cells, and unsaturated disaccharides were produced by enzymatic digestion and then separated by reversed-phase ion-pairing HPLC and reacted with 2-cyanoacetamide to form derivatives for fluorescence detection.[30] Dermatan sulfates were estimated by measuring unsaturated disaccharides with chondroitinase ACII digestion compared with both ACII and ABC. Unsaturated disaccharides from hyaluronan were determined with fluorometric postcolumn HPLC with graphitized carbon column as reported previously.[31]

Measurement of Proteoglycan-Related Gene Expression Levels using Quantitative RT-PCR (qRT-PCR). Primer Design and Validation. Primer pairs for GAG-related genes and control genes were designed within a single exon using conditions described in Nairn et al. (in preparation). Primers were validated using the standard curve method[32] with dilutions of mouse genomic DNA as template. Only primer pairs, which gave efficiencies of 100 ± 10% with genomic DNA, were considered as validated for further experiments. Primer sequences and accession numbers for genes in this study are presented in Supplementary Table 1. Individual qRT-PCR reactions were also checked for efficiency 100 ± 5% using reaction raw fluorescence data in the LinReg PCR program.[33]

Total RNA Isolation and cDNA Synthesis. mESC, EB, and ExE cell pellets were harvested and flash frozen in liquid nitrogen and stored at −80 °C until use. Cell pellets were homogenized using a polytron, and RNA was isolated using Trizol Reagent (Invitrogen) and Phase Lock Gel (Eppendorf) following manufacturer instructions. Total RNA was precipitated using LiCl (2.5 M final concentration), resuspended in RNase-free water and treated with RNase-free DNase (Ambion) to remove genomic DNA. Samples were re-extracted with Trizol then reprecipitated with LiCl and resuspended in RNase-free water and used for cDNA synthesis. One microgram of total RNA was used for a 20 μL cDNA synthesis reaction using the SuperScript III First-Strand Synthesis System (Invitrogen). Reactions were diluted 1:10 with DEPC-treated water prior to qRT-PCR assays.

qRT-PCR Reactions. Triplicate reactions (20 μL each) containing 5 μL of diluted cDNA or genomic DNA template, 5 μL of primer pair mix (125 μM final concentration), and 10 μL of iQ SYBR Green Supermix (BioRad) were assembled in 96 well microtiter plates. Plates were sealed with optical film and centrifuged at 2500 rpm for 5 min before being placed into a MyiQ or iCycler Real Time PCR machine (BioRad) using the following cycling conditions: 95 °C for 3 min, followed by 40 cycles of: 95 °C for 10 s (denaturing), 65 °C for 45 s (annealing), and 78 °C for 20 s (data collection). Following the thermal cycling and data collection steps, amplimer products were analyzed using a melt curve program (95 °C for 1 min, 55 °C for 1 min, then increasing 0.5 °C per cycle for 80 cycles of 10 s each). The control gene, Ribosomal Protein L4 (RPL4, NM_024212), was included on each plate to control for run variation and to normalize individual gene expression.

Calculation of Relative Gene Expression Levels. Triplicate Ct values for each gene were averaged, and the standard deviation was calculated. Samples that resulted in a standard deviation of >0.5 Ct units were rerun until values with standard deviations within an acceptable range were acquired. The logarithmic average Ct value for each gene and the control gene was converted to a linear value using the conversion: 2^{-Ct}. Converted values were normalized to RPL4 by dividing the individual gene value by the control gene value. Normalized values were scaled so that genes that were below the level of detection were given a value of 1×10^{-6}, and this value was used as the lower limit on histograms.

Results

Characterization of mESCs, EBs, and ExE. Differentiation of mESCs over 4 days into embryoid bodies reveals gross morphological changes (Figure 2A) and produces a heterogeneous population of cells including extraembryonic endoderm (ExE) and varying amounts of the three embryonic germ layers: ectoderm, mesoderm and embryonic endoderm. Increases in transcript abundance for an ectoderm marker (Zic1), a mesoderm marker (goosecoid (GSC)), and embryonic endoderm markers (Sox17, AFP, and GATA-6) were observed in the EB population demonstrating the presence of all three germ layers (Figure 2B) in addition to similar or slightly reduced amounts of transcripts for pluripotency markers (Zfp42(Rex1),-GBX2 and Nanog). In contrast, treatment of mESCs with RA generates primarily ExE, as indicted by >10-fold increases in Sox17, AFP, and GATA-6 transcript levels. Consistent with loss of pluripotency, RA-treated cells show a decrease in transcript abundances of ESC markers Zfp42 (Rex1), GBX2, and Nanog (Figure 1B).

Disaccharide Analysis of GAGs from mESC, EBs, and ExE. A mESC line, grown under feeder-free conditions, EBs, and ExE generated from this cell line were used to study the GAG glycome. mESCs, EBs, and ExE cells (10^7 cells from R1 cell line) were freeze-dried, and the GAGs were recovered. Treatment of these GAGs with selected polysaccharide lyases afforded their constituent disaccharide components (Figure 1), which were analyzed by RPIP-HPLC with postcolumn fluorescence detection affording high-resolution chromatograms (not shown). Assignment of peaks was performed by co-injection of authentic disaccharide standards, and quantification was obtained from standard curves. Tables 1 and 2 show the disaccharide composition of the mESCs, EBs, and ExE cell lines, as well as the total amount of each type of GAG present in these cell lines.

Hyaluronan (HA) showed a 13- and 24-fold increase when mESCs differentiated to ExE and EB cells, respectively. The total CS/DS biosynthesized by EBs and ExE cells was 4- and 6-fold higher, respectively, than that synthesized by mESCs. The most prominent change in CS/DS composition of both EBs and ExE was a decrease in 6S disaccharide (CS_C + DS_C) with a concomitant increase in 4S,6S (CS_E) disaccharide. Other changes observed include an increase in 4S,6S (DS_E) and 2S,4S (DS_B) in

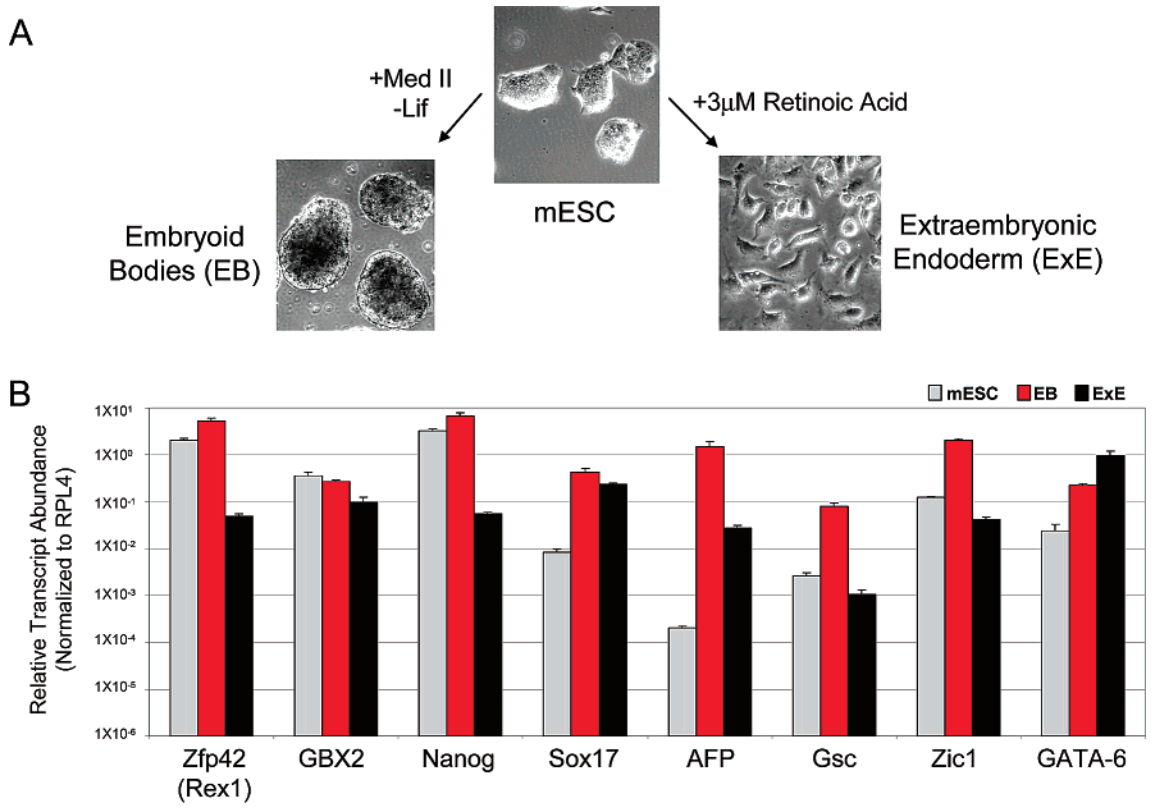

Figure 2. Characterization of mESC, EBs, and ExE cell populations. (A) Phase contrast images demonstrating the morphological differences between mESC, EBs, and ExE cell populations. (B) Transcript analysis of genes for pluripotent (mESC) markers [(Zinc finger protein 42 (Zfp42/Rex1), Gastrulation brain homeobox 2 (GBX2), and Nanog homeobox (Nanog)] and differentiation markers [SRY-box containing gene 17 (Sox17), Alpha fetoprotein (AFP), Goosecoid (Gsc), Zinc finger protein of the cerebellum 1 (Zic1), and GATA binding protein 6 (GATA-6) in total RNA isolated from mESCs, EBs, and ExE were performed as follows: Average Ct values from triplicate samples obtained for each gene, with a standard deviation of less than 0.5 Ct units, were converted to linear values and normalized to the housekeeping gene RPL4 (as described in Materials and Methods). Relative transcript abundance for mESC (gray bars) and EB (red bars) and ExE (black bars) are plotted on a log scale for each gene assayed. Error bars represent 1 standard deviation from the mean. Transcript values less than 1×10^{-6} are below the threshold of detection.

Table 1. Hyaluronan and Chondroitin/Dermatan Sulfate Content and Disaccharide Analysis CS and/or DS (Unsaturated Disaccharide, %)[a]

			none[c]	4S		6S	2S[e]	4S6S[e]		2S4S[e]		2S6S[e]		triS[e]
			CS+DS[d]	CS	DS	CS+DS	CS+DS	CS	DS	CS	DS	CS	DS	CS+DS
cell type	total[b] HA	total[b] CS+DS	(0S)[c]	(CS_A)	(DS_A)	(CS_C,DS_C)	(UA2S)	(CS_E)	(DS_E)	(CS_B)	(DS_B)	(CS_D)	(DS_D)	
mESC	0.7	2.7	11.6	20.8	52.2	15.4	N.D.	N.D.	N.D.	N.D.	N.D.	N.D.	N.D.	N.D.
EB	17.2	11.8	21.6	37.6	26.7	11.3	N.D.	2.8	N.D.	N.D.	trace	N.D.	trace	N.D.
ExE	9.5	16.0	9.8	29.0	47.5	3.6	N.D.	2.9	5.5	N.D.	1.7	N.D.	trace	N.D.

[a] The degree of sulfation calculated from the disaccharide analysis was 0.88 sulfo groups/disaccharide for mESC, 0.81 sulfo groups/disaccharides for EB, and 1.00 sulfo/groups/disaccharide for ExE. [b] Totals determined as ng/10^6 cells. [c] Position of sulfo groups added as shown in Figure 1. Abbreviations for CS and DS disaccharides used in Figure 1 throughout the text. [d] GAG analyzed, where the amount of CS and DS could not be determined separately are shown as "CS+DS". [e] N.D. = none detected.

ExE. The total HS biosynthesized by EBs and ExE was 5- and 8-fold higher, respectively, than that synthesized by mESCs. Both EBs and ExE showed substantial increases in the HS disulfated disaccharide sequence, NS6S. The ExE cells biosynthesized 2-fold more HS trisulfated disaccharide, 2SNS6S, than did mESC.

Quantitative Analysis of mRNA Expression. The relative expression of genes involved in GAG biosynthesis, modification, and catabolism, as well as core proteins, were next determined for mESC cells, EB cells, and ExE cells using a newly developed array of primers and quantitation by qRT-PCR.

Transporter Proteins and Enzymes Involved in Precursor Biosynthesis. Six precursors, PAPS, UDP-GlcNAc, UDP-GalNAc, UDP-GlcA, UDP-Xyl, and UDP-Gal, are important in the biosynthesis of the uronic acid containing GAGs, HS, CS/DS, and HA (Figure 3A). The relative level of gene expression in mESC, EB, and ExE cells were determined for a number of transporter and biosynthetic proteins involved in the uptake and biosynthesis of these precursors. Transcript abundance for most genes involved in the synthesis of GAG precursors (Figure 3B) were unchanged, slightly down-regulated, or slightly up-regulated both in EB and ExE cells, as compared to undifferentiated mESCs. One exception was hexokinase isoform 3, which is approximately 30-fold up-regulated in both EB and ExE cells. The results from the gene expression studies on these proteins involved in the early steps of GAG biosynthesis could

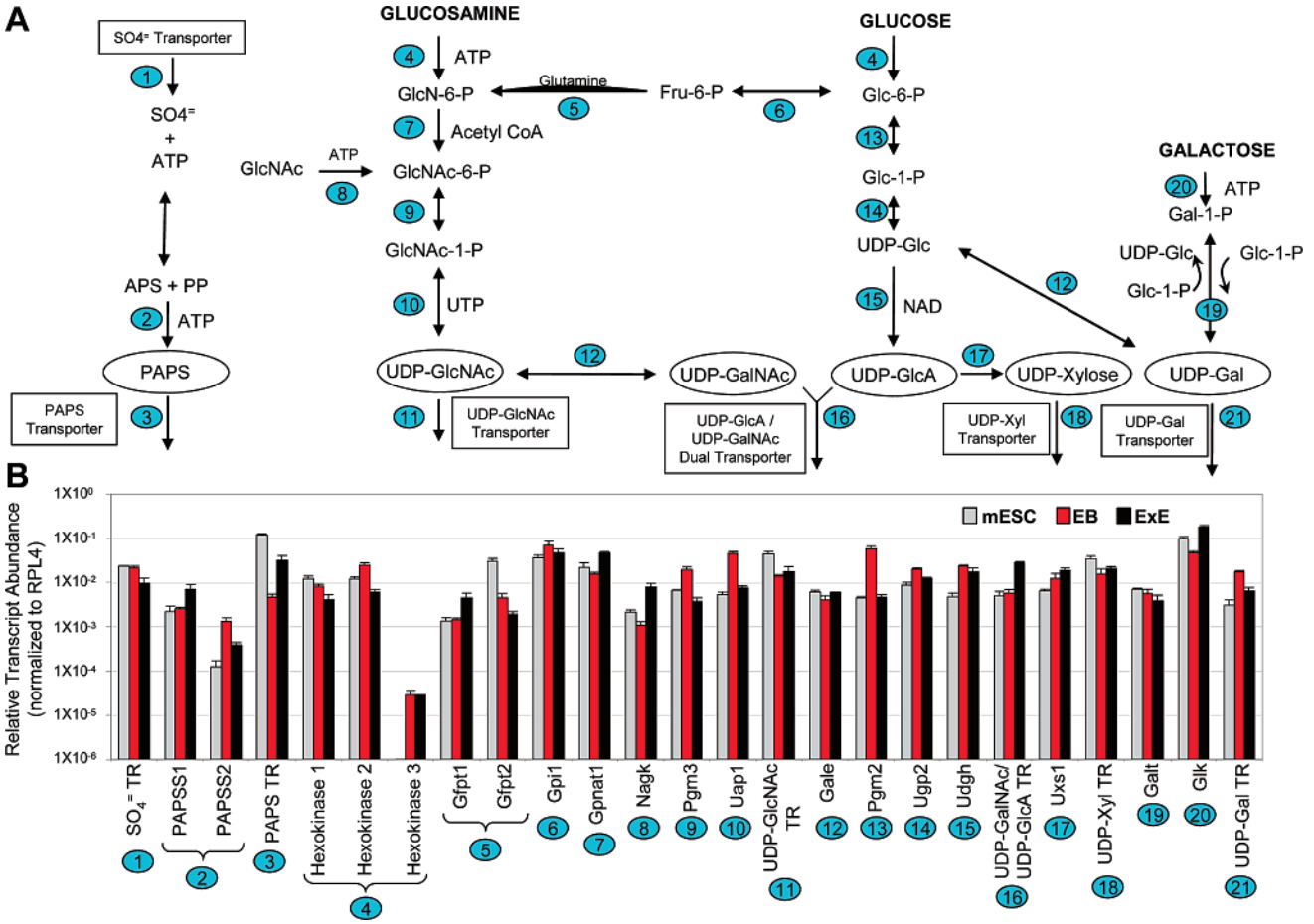

Figure 3. Precursors important in the biosynthesis of uronic acid containing GAGs. (A) The immediate precursors of GAG biosynthesis are shown in ovals and transporter proteins are shown in rectangles. Biosynthetic reactions and transporter proteins are numbered 1−21 in small blue ovals. (B) Expression of genes involved in the synthesis of precursors of GAG biosynthesis and transporter proteins 1−21: 1. Sulfate anion transporter (SO_4 = TR); 2. PAPS synthase-1 and -2 (PAPSS1, PAPSS2); 3. PAPS transporter (PAPS TR); 4. Hexokinase 1, 2 and 3; 5. Glutamine fructose-6-phosphate transaminase-1 and -2 (Gfpt1, Gfpt2); 6. Glucose-6-phosphate isomerase (Gpi1); 7. Glucosamine-phosphate N-acetyltransferase 1 (Gpnat1); 8. N-acetylglucosamine kinase (Nagk); 9. Phosphoglucomutase 3 (Pgm3); 10. UDP−N-acetylglucosamine pyrophosphorylase 1 (Uap1); 11. UDP-GlcNAc transporter (UDP-GlcNAc TR); 12. UDP-galactose-4-epimerase (Gale); 13. Phosphoglucomutase 2 (Pgm2); 14. UDP-glucose pyrophosphorylase 2 (Ugp2); 15. UDP-Glucose dehydrogenase (Udgh); 16. UDP-GalNAc and UDP-GlcA dual transporter (UDP-GalNAc/UDP-GlcA TR); 17. UDP-glucuronate decarboxylase 1 (Uxs1); 18. UDP-Xylose transporter (UDP-Xyl TR); 19. Galactose-1-phosphate uridyl transferase (Galt); 20. Gluco/galactokinase (Glk); and 21. UDP-Gal transporter (UDP-Gal TR). Transcript analysis of indicated genes in total RNA isolated from mEB and were performed as follows: Average Ct values from triplicate samples obtained for each gene, with a standard deviation of less than 0.5 Ct units, were converted to linear values and normalized to the housekeeping gene RPL4 (as described in Materials and Methods). (B) Relative transcript abundance for mES (gray bars) and (red bars) and (black bars) are plotted on a log scale for each gene assayed. Error bars represent 1 standard deviation from the mean. Transcript values less than 1×10^{-6} are below the threshold of detection.

Table 2. Heparan Sulfate Content and Disaccharide Analysis

cell type	total HS (ng/10^6cell)	HS (unsaturated disaccharide, %)[a]							
		NAc[b]	NS	NAc6S	2SNAc	NS6S	2SNS	2SNAc6S	2SNS6S
mESC	12.1	60.5	18.2	4.5	0.8	2.6	10.2	0.0	3.2
EB	57.5	59.1	17.5	6.1	0.4	4.2	10.6	0.0	2.1
ExE	93.9	49.3	22.4	6.9	0.8	4.8	8.9	0.0	6.9

[a] The degree of sulfation calculated from the disaccharide analysis was 0.66 sulfo groups/disaccharide for mESE, 0.60 sulfo groups/disaccharide for EB, and 0.78 sulfo groups/disaccharide for ExE. [b] Abbreviations for HS disaccharide used in Figure 1 and throughout the text.

not explain the observed increase in GAG content resulting from ESC differentiation, suggesting that adequate precursor pools are present in the cells for the large enhancement in GAG biosynthesis, which occurs when mESCs differentiate to EBs and ExE.

Enzymes Involved in HA Biosynthesis and Catabolism. HA, the structurally least complex of the GAGs, is biosynthesized at the cell membrane, by hyaluronan synthases −1, −2, and −3 (Has1, Has2, and Has3, respectively) (Figure 4A). HA is then catabolized at the cell membrane and intracellularly to smaller bioactive polysaccharides and oligosaccharides through the action of six hyaluronidases, encoded by two sets of three tightly clustered genes, Hyal-1, Hyal-2, and Hyal-3 and Hyal-4, PH-20, and Hyal-5 (Figure 4). Transcript levels for genes involved in HA biosynthesis and catabolism were examined (Figure 4B). HA synthase 2 (Has2) transcript levels were >200- and >3000-fold up-regulated in ExE and EB cells, respectively. Has1 transcript abundance was also increased by approximately 50- and 5-fold in ExE and EB cells, respectively. These

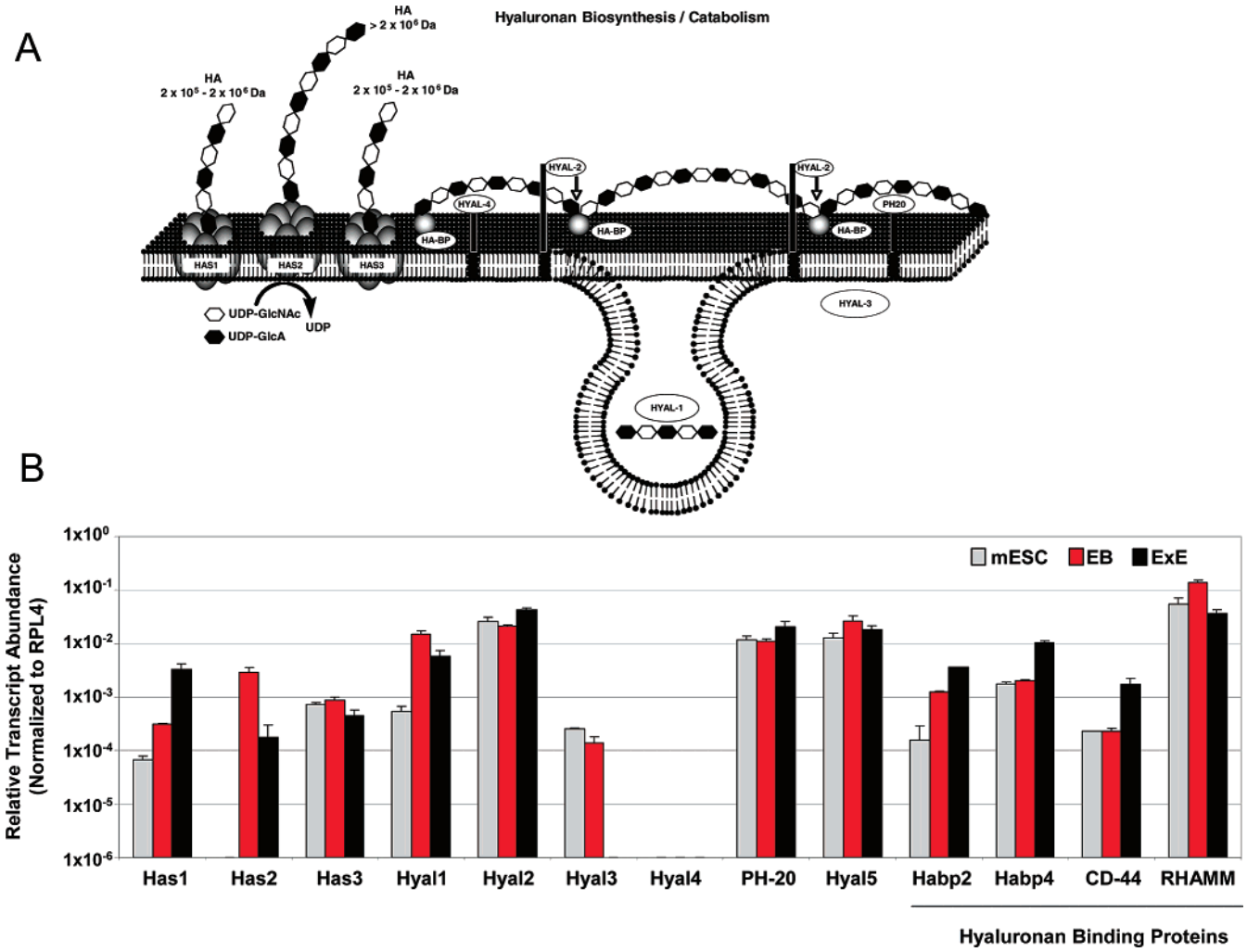

Figure 4. Hyaluronan biosynthesis and catabolism. (A) Biosynthesis takes place at the plasma membrane through the action of hyaluronan synthases (Has1−3) on UDP-GlcNAc and UDP-GlcA. Intermediate (200−1000 kD) and long (1000 kD) chains of HA are extruded out of the cell and anchored on the external membrane surface through hyaluronan binding proteins (HA-BPs). The membrane-bound HA is then catabolized into smaller bioactive chains at the cell membrane through the action of GPI-anchored hyaluronidases (Hyal2, Hyal4, and PH20) and within the cell through the action of Hyal1 and Hyal3. (B) Expression of genes involved in HA synthesis and catabolism. Transcripts examined are as follows: Hyaluronan synthase-1 (Has1), Hyaluronan synthase-2 (Has2), Hyaluronan synthase-3 (Has3), Hyaluronidase-1 (Hyal1), Hyaluronidase-2 (Hyal2), Hyaluronidase-3 (Hyal3), Hyaluronan glucosaminidase-4 (Hyal4), PH-20, Hyaluronidase-5 (Hyal5), Hyaluronic acid binding protein 2 (Habp2), Hyaluronic acid binding protein 4 (Habp4), CD-44, and RHAMM. Relative transcript abundance for mESC (gray bars) and EB (red bars) and ExE (black bars) are plotted on a log scale for each gene assayed. See legend of Figure 2 for details.

changes clearly correlate well with the increase in amount of HA isolated from these cell types (Table 1). The transcripts for genes involved in HA catabolism show different trends. Transcripts for Hyal1 were increased, whereas transcripts for Hyal2, Hyal4, Hyal5, and PH-20 were unchanged, and Hyal3 transcript levels were unchanged in EBs but down-regulated (>100-fold) in ExE.

Transcript levels of HA binding proteins, residing on the cell surface, were also determined. CD-44 and Habp4 transcripts increased modestly only in ExE, while Habp2 transcript levels increased by ~8-fold in EBs and >20-fold in ExE as compared to mESCs. RHAMM transcripts increased slightly in EBs and decreased slightly in ExE, when compared to levels in mESCs. These observed differences, in the transcript levels of Habp2, Habp4, and CD-44, suggest that stem cells may preferentially utilize different HA binding proteins to anchor HA.

Expression of transcripts encoding Core Proteins Carrying GAG Chains. Whereas HA is biosynthesized as a free polysaccharide, CS/DS and HS are biosynthesized on a protein core (Table 3). The expression of a number of core proteins was examined in mESCs, EBs, and ExE (Figure 5). CS/DS core proteins, with increased transcript levels (by ~10-fold or more) in both EB and ExE, included versican, decorin, biglycan, and thrombomodulin. Transcript levels of tenascin-C and epican increased 200- and 10-fold only in ExE. Neuroglycan transcript levels decreased slightly (<10-fold) in EBs and ExE. Epiphycan decreased (by 1000-fold) in ExE compared to ESCs, and the levels in EBs and mESCs were similar. RPTP beta/phosphocan transcript levels increased by ~15-fold in EBs but decreased by ~10-fold in ExE, when compared to ES cells. HS core proteins with increased expression levels (by ~10-fold or more) in both EBs and ExE included glypican 3, glypican 6, and collagen XVIII. Transcript levels for perlecan, syndecan 2, and syndecan 3 increased (by ~10-fold) in ExE compared to ESCs. Glypican 5 transcript abundance increased (by >100-fold) in EBs compared to ESCs. In summary, core protein transcript

Table 3. Proteoglycan Core Proteins[85−89]

	isoforms	GAGS	#GAG chains
Agrecan 1 (CSPG1)	1	CS	100
Versican (CSPG2)	1	CS	10−30
Neurocan (CSPG3)	1	CS	3−7
NG2 (CSPG4)	1	CS	1
Neuroglycan (CSPG5)	1	CS	1−7
Bamacan	1	CS	3
Brevican (CSPG7)	1	CS	1−3
Decorin	1	DS/CS	1
Biglycan	1	DS/CS	2
Procollagen 1Xa2	1	CS	1
Thrombomodulin	1	CS	1
Epican (CD44)	1	CS	1
CD74	1	CS	1
RPTP beta/phosphacan	1	CS	3−4
Tenascin-C	1	CS	0−4
Tenascin-R	1	CS	1
Asporin	1	CS	0−2
Epiphycan DSPG	1	DS/CS	2−3
Serglycin	1	HP/CS_E	7−15
Perlecan	1	HS/CS	3
Agrin	1	HS	3
Syndecan	4	HS	2−5
Glypican	6	HS	2
Collagen XVIII	1	HS	1

levels generally increased or remained constant in both the CS/DS and HS proteoglycan families.

Expression of Enzymes Involved in Common Linkage Region Sequence. The first four steps of the synthesis of GAG chains linked to core proteins, CS/DS, and HS share a common pathway (Figure 6A) involving xylosyl transferase (Xylt1 and Xylt2), β4-galactoslytransferase (β4galt7), β3-galactosyltransferase (β3galt6), and β3-glucuronosyltransferase (β3gat1, β3gat2, β3gat3). The transcript levels for four of these enzymes all showed only slight differences, with the interesting exception of the transcript encoding β3-glucuronosyltransferase I (β3gat1), which showed a 100-fold decrease on differentiation of mESCs to ExE (Figure 6B). The change observed in transcript levels for β3gat1 is currently unclear but suggests that it may be important to examine the subspecificity of the β3-glucuronosyltransferase isoforms.

Expression of Enzymes Involved in Late Linkage Region Biosynthesis and Chain Extension. HS linkage region biosynthesis and chain extension requires α4-GlcNAc transferase (Extl2 and Extl3), glucuronsyltransferase (Ext1,Ext2) and combined GlcAT and GlcNAcT activities (present in copolymerase Ext1/Ext2, Extl1 and Extl3) (Figure 6A). Of all the chain extension enzymes in HS biosynthesis, only Extl1 transcript abundance show a substantial change, decreasing by ∼40-fold upon differentiation of mESC to ExE cells (Figure 6B).

CS/DS linkage region biosynthesis and chain extension require two additional enzymatic activities, β4-GalNAc transferase (GalNAct2), and chondroitin synthase (Chsy1, Chsy2, Chsy3-like), which has both β3GlcAT and β4GalNAcT activities required to form the repeating disaccharide (Figure 6A). Of all the chain extension enzymes in CS/DS biosynthesis, only Chys3-like transcript levels show a substantial change, increasing 5- and 50-fold in EBs and ExE, respectively (Figure 6B). Chondroitin is converted to dermatan via epimerization of GlcA to iduronic acid (IdoA) which is accomplished by dermatan sulfate epimerase (Dse and Dsel). Expression of Dse was fairly constant for all cell types whereas Dsel expression increased ∼10-fold in EBs compared to mESCs.

Expression of Enzymes Involved in the Modification of HS GAG Repeating Unit. HS *N*-deacetylase, *N*-sulfotransferase isoforms 1−4 (NDST1, NDST2, NDST3, and NDST4), HS 5′-uronosyl epimerase (Glce), HS 2-*O*-sulfotransferase (Hs2st1), HS 6-*O*-sulfotransferase isoforms 1−3 (Hs6st1, Hs6st2, Hs6st3), and HS 3-*O*-sulfotransferase isoforms (Hs3st1, Hs3st2, Hs3st3a1, Hs3st3b1, Hs3st5, and Hs3st6) are involved in the modification of the HS GAG repeating unit (Figure 7A). NDST-1 transcript levels slightly increased (by <10-fold), whereas NDST-2 transcript levels increased (by ∼10-fold in both EBs and ExE) (Figure 7C). NDST-3 and NDST-4 show increased expression levels only in EBs. The transcript levels of C5Epi(Glce) and Hs2st1 remained relatively unchanged. The transcript levels of Hs6st2 increased for both EBs and ExE (100-fold and 500-fold, respectively), whereas Hs6st1 remained relatively unchanged and the Hs6st3 increased by ∼20-fold on mESC differentiation to ExE. HS 3-*O*ST isoform 3a1 transcript (Hs3st3a1) increased (∼300-fold and ∼600-fold, respectively) for both EBs and ExE, while 3-*O*ST isoform 1 transcript (Hs3st1) increased ∼40-fold only for ExE and the 3-*O*ST isoform 2 transcript Hs3st2 increased ∼30-fold only for EBs.

Expression of Enzymes Involved in the Modification of CS/DS GAG Repeating Unit. Several enzymes are involved in the modification of the CS/DS GAG repeating unit (Figure 7B) and are specific for the addition of sulfates to GlcA/IdoA (2S) or GalNAc (4S and/or 6S). Chondroitin uronosyl sulfotransferase (Ust) adds sulfate to the GlcA residue of chondroitin or the IdoA residue of dermatan. Transcripts for Ust were ∼60-fold more abundant for EB and ExE cells.

Chondroitin 4-*O*-sulfotransferase (Chst11 and Chst12) and Dermatan 4-*O*-sulfotransferase (D4st1) add sulfate to the 4-*O* position of GalNAc in chondroitin and dermatan, respectively. Expression of both isoforms of Chondroitin 4-*O*ST (Chst11 and Chst12) are elevated slightly in ExE (∼5-fold) and D4st1 expression is more elevated in ExE (∼10-fold) as compared to mESCs, whereas expression of these enzymes is similar between mESCs and EBs.

Addition of sulfate to the 6-*O* position of GalNAc on chondroitin or dermatan can be accomplished by chondroitin 6-*O*-sulfotransferase (Chst3 and Chst7) or *N*-acetylgalactosamine 4S,6S transferase (GalNAc 4S6ST). Expression of one 6-*O*ST isoform, Chst3, is relatively similar for all cell types, whereas expression of the other isoform, Chst7, is increased by ∼10-fold in both EBs and ExE, compared to mESCs. GalNAc4S6ST transcript abundance increased ∼40-fold in EBs and ∼25-fold in ExE compared to mESCs (Figure 7C). This upregulation presumably resulted in the increase of CS/DS 4S,6S (S_E) and CS/DS 2S,4S (S_B) structures (Table 1).

Discussion

A prominent finding of this study is the increased biosynthesis of all of the uronic acid containing GAGs, upon differentiation of mESCs to EBs and ExE. This result suggests that the biosynthesis and transport of the GAG precursors PAPS, GlcA-UDP, GlcNAc-UDP, GalNAc-UDP, Gal-UDP, and Xyl-UDP may all be enhanced in EB and ExE cells (Figure 3). Contrary to our expectations, the transcript levels of most of these transporters and biosynthetic enzymes remained unchanged on differentiation. It is likely that the pools of these precursors are sufficient to allow the 4- 24-fold increase in GAG synthesis observed on differentiation of mESCs to EBs and ExE. Although precursor transporters and biosynthetic enzymes are clearly essential for GAG biosynthesis,[34] they do not appear useful in predicting GAG levels within the ranges encountered in the current study.

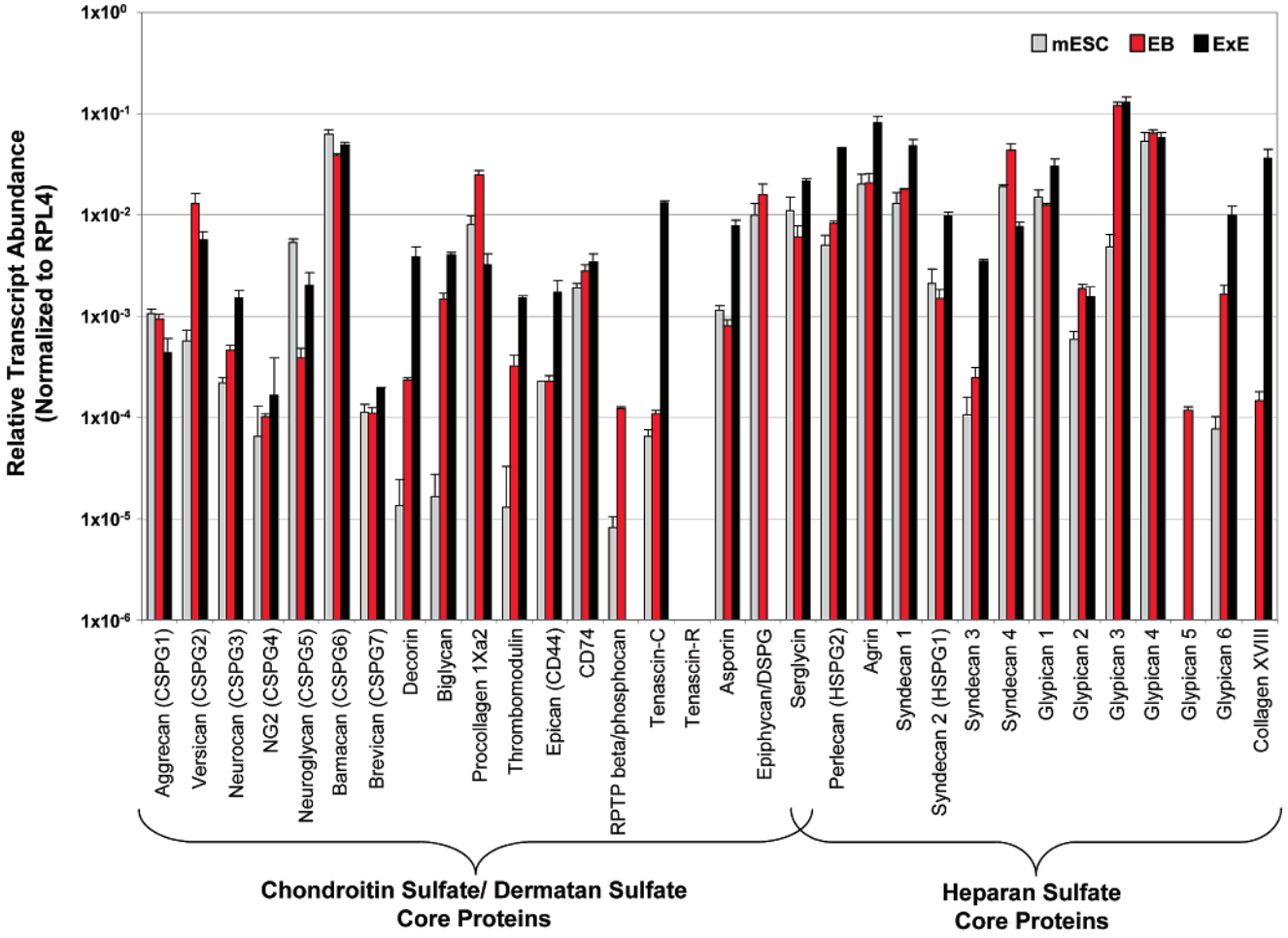

Figure 5. Biosynthesis of chondroitin/dermatan sulfate and heparan sulfate core proteins. The relative transcript abundance of mRNAs for CS/DS core proteins aggrecan (CSPG1), versican (CSPG2), neurocan (CSPG3), NG2 (CSPG4), neuroglycan (CSPG5), bamican (CSPG6), brevican (CSPG7), decorin, biglycan, procollgen, thrombomodulin, epican, CD74, RTP beta/phosphocan, tenascin-C, tenascin-R, asporin, and epiphycan and the mRNA for the HS core proteins, perlecan, agrin, syndecan1−4, glypican1−6, and collagen XVIII were determined. Relative transcript abundance for mESC (gray bars) and EB (red bars) and ExE (black bars) are plotted on a log scale for each gene assayed. See legend of Figure 2 for details.

HA is biosynthesized through the action of three Has isoforms and catabolically processed through the action of six Hyal isoforms (Figure 4A). Because HA has a uniform repeating unit, contains no core protein, and is not sulfated, it is believed to show differential activity based on chain length.[35] Thus, the expression levels of both biosynthetic and catabolic enzymes were examined. Transcripts for two of the three Has isoforms were at higher levels in EBs and ExE, suggesting an explanation for the 13- and 24-fold enhancement of HA levels in ExE and EB cells, respectively. Although mammalian Has enzymes have distinct catalytic properties,[36] it is unclear why there are three Has isoforms because they all appear to be independently active. Has2, with transcript levels enhanced by 200- and 3000-fold in ExE and EBs, respectively, synthesizes the highest molecular weight ($>10^6$ Da) HA.[37] Experiments using histochemical staining of cultured tissue fragments from mouse embryos revealed that HA was detected in early stages of ExE cell cultures.[38] A knock out study of the Has2 gene demonstrated that the Has2 product was critical for embryogenesis. In contrast, overexpression of Has2 enhanced anchorage-independent growth and tumorgenicity.[39] HA shows an extraordinary rate of turnover in mammals and has an intravenous $t_{1/2}$ of 2−5 min in rabbits.[40] HA is biosynthesized at the cell membrane, extruded through the membrane and anchored on the external membrane surface of the cell by HA binding proteins. The transcript levels for these binding proteins are different in both EBs and ExE. It is on the outer membrane of the cell that catabolic processing of HA occurs through the action of hyaluronidases (Hyal). There are six Hyal genes arranged in two three-gene clusters.[41] Hyal1 and Hyal2 constitute the major hyaluronidase in somatic tissues. A null mutation in Hyal2 in mouse is embryonic lethal whereas mutations in Hyal1 result in mucopolysaccharidosis.[42] Hyal3, with decreased transcript levels in ExE, does not show enzymatic activity using currently available hyaluronidase assays,[41] but its expression is observed in chondrocytes[43] and increases when fibroblasts undergo chondrocyte differentiation.[44] Hyal4 appears to be a chondroitinase, but no detectable expression of this gene was observed in any of the cell types assayed. Finally, PH-20 (SPAM1), showing similar levels in all cell lines, facilitates penetration of sperm through the cumulus surrounding the ovum in fertilization[45] and binds through a separate domain to the zona pelucida.[46] PH-20 has been detected in fetal tissues[47] and in malignancies.[48] In summary, despite the homogeneous repeating structure of HA, stem cells may control its size through the differential expression of Has or Hyal isoforms or may restrict its localization through controlling the expression of HA binding proteins.

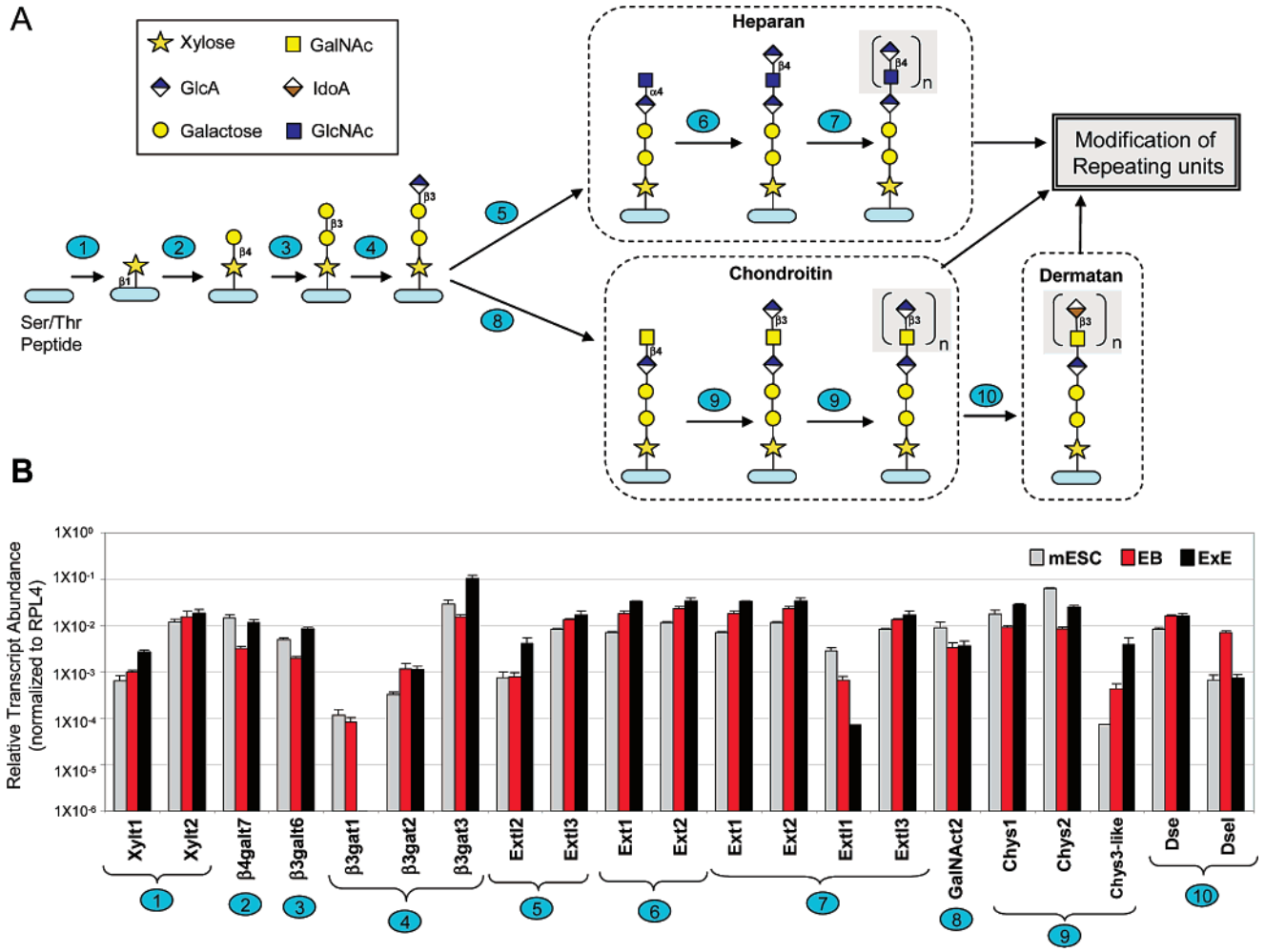

Figure 6. Biosynthesis of chondroitin/dermatan sulfates and heparan sulfate core structures. (A) The core protein (Ser/Thr containing polypeptide shown in light blue) is glycosylated and modified in the endoplasmic reticulum and Golgi through 10 enzymatic reactions (numbered blue ovals). The linkage region tetrasaccharide common to both CS/DS and HS is synthesized first [reactions 1−4]. A xylose residue (yellow star) is transferred through the action of xylosyltransferase-1 or -2 (Xylt1, Xylt2) to Ser through a *β-O*-glycosidic linkage [reaction 1]. Galactose (yellow circle) is *β*-linked to the 4-position of Xyl through the action of the *β*-4 galactosyltransferase (*β*4galt7) [reaction 2] followed by addition of *β*3-linked galactose through the action of *β*-3 galactosyltransferase (*β*3galt6) [reaction 3] and glucuronic acid (blue and white diamond) is *β*3-linked through the action of *β*-3-glucuronosyl transferase (*β*3gat1, *β*3gat2, *β*3gat3) [reaction 4]. The biosynthesis of CS/DS and HS families diverge in the chain extension and modification steps. The HS biosynthetic pathway is committed with the transfer of α4-linked *N*-acetylglucosamine (blue square) through the action of α-*N*-acetylglucosaminyltransferases ExtI2 and ExtI3 [reaction 5]. The HS polysaccharide chain is extended through the action of α-*N*-acetylglucosaminyl-*β*-glucuronosyl transferases Ext1 and Ext2 [reaction 6], followed by disaccharide polymerization via the concerted action of Ext1, Ext2, ExtI1, and ExtI3 [reaction 7]. The CS/DS biosynthetic pathway is committed with the transfer of *β*4-linked *N*-acetylgalactosamine (yellow square) through the action of *β*-*N*-acetylgalactosaminyltransferase (GalNAct2) [reaction 8]. The polysaccharide chain is extended through the action of *β*-*N*-acetylgalactosaminyl-*β*-glucuronosyl transferases (Chys1, Chys2, and Chys3-like) [reaction 9]. The glucuronic acid residue in dermatan sulfate is C_5 epimerized to iduronic acid (white and brown diamond) through the action of DS epimerase (Dse and Dsel) [reaction 10]. Further modifications of the disaccharides (shown in gray squares) for HS, CS and DS are shown in Figure 6. (B) Expression of genes involved in the biosynthesis of the linkage region and chain extension corresponding to the reactions in (A) are shown. Relative transcript abundance for mESC (gray bars) and EB (red bars) and ExE (black bars) are plotted on a log scale for each gene assayed. See legend of Figure 2 for details.

Next, we looked at the biosynthesis of a wide array of CS/DS and HS core proteins (Table 3). Many studies have examined proteoglycan synthesis in mid-stage to late stage embryos,[49] but little is known about the proteoglycans of the pre-implantation stages of embryogenesis. Syndecan 1 is known to appear at the four-cell stage[50] and perlecan in day 4 blastocysts.[51,52] Serglycin is synthesized and secreted by ES cells.[49] Retinoic acid treatment of ES cells (affording ExE) results in slight enhancement of serglycin mRNA levels. ExE cell markers include laminin and collagen IV, major components of the basement membrane formed by ExE cells.[52]

Proteoglycan core transcript levels in mESCs, EBs, and ExE cells were next examined. Our results may explain the enhanced production of CS/DS and HS GAGs, as the transcript level of core proteins increased (by >10-fold) in 39% of the cases, remained unchanged (<10-fold change) in 56% of the cases, and decreased (by >10-fold) in 3% of the cases on mESC to EB and ExE differentiation. In the hyalectin family (HA-binding proteoglycans that include aggrecan, versican, neurocan and brevican), only versican showed major enhancement of transcript levels on mESC differentiation to EBs and ExE (Figure 5). Versican expression and regulation is controlled by

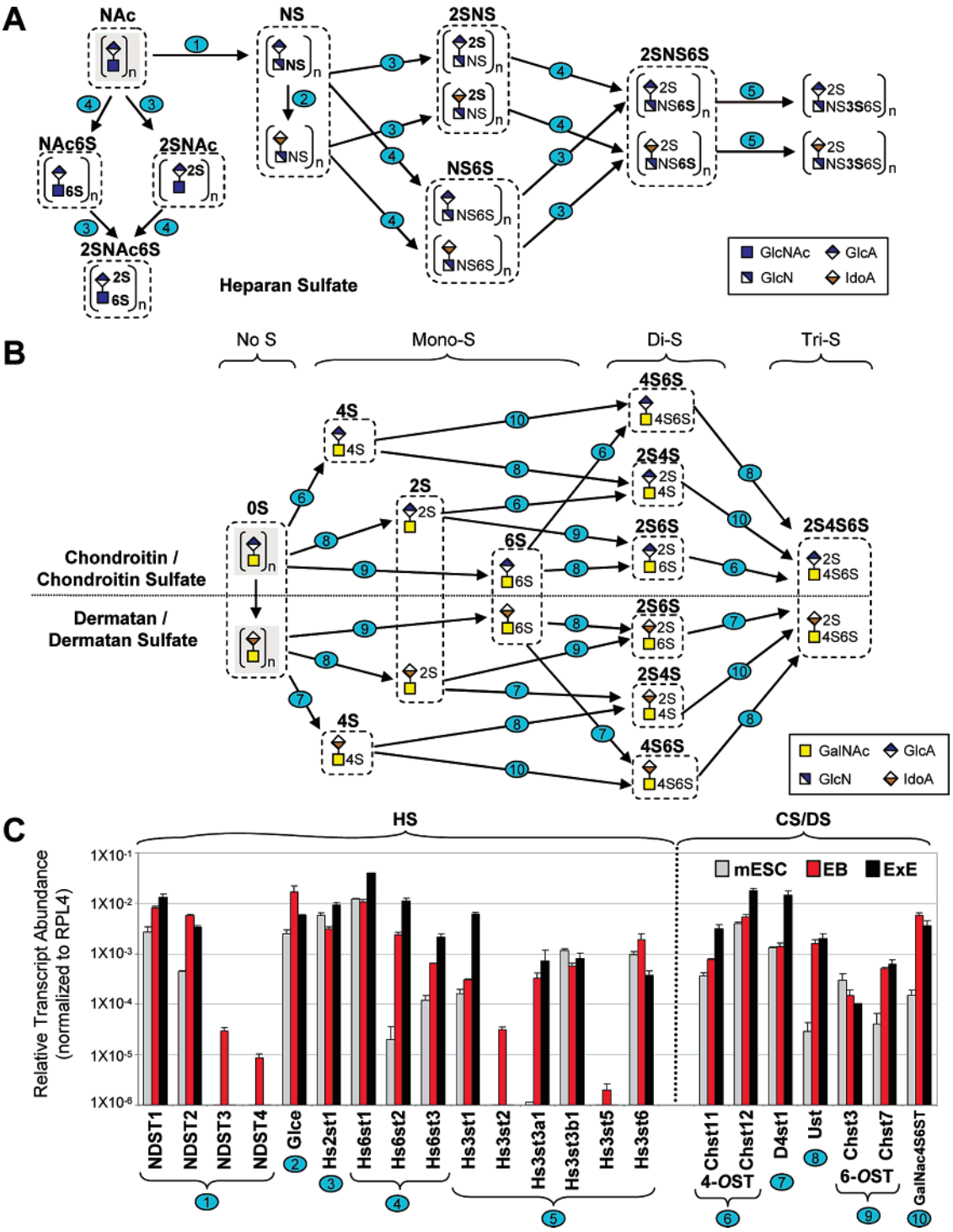

Figure 7. Modification of heparan sulfate and chondroitin/dermatan sulfate repeating units. (A) Synthesis of HS. Selective action of *N*-deacetylase, *N*-sulfotransferases (NDST1−4) afford *N*-sulfated (NS) glucosamine (blue and white square) residues [reaction 1]. Selective action of C_5 Epimerase (Glce) converts some GlcA residues (blue and white diamond) to IdoA residues (white and brown diamond) [reaction 2]. Selective modification of uronic acids by 2-sulfo transferase, Hs2st1 (2S) [reaction 3] and selective modification of GlcN residues by 6- and 3-*O*-sulfation (6S and 3S, respectively) through the action of Hs6st1−3 and Hs3st1,2,3a1,3b1,5,6 [reactions 4(6S) and 5(3S)]. The abundance of the disaccharide structures enclosed in dotted lines were determined and the corresponding data is shown in Table 2. (B) Synthesis of CS and DS. The 4-position of *N*-acetylgalactosamine (4S) of chondroitin is sulfated by Chst11 or Chst12 [reaction 6] and the same position of dermatan is sulfated by D4st1 [reaction 7]. Subsequently the 4S sulfated product is sulfated at the 6-position by GalNAc4S6ST producing a disulfated product (4S6S) [reaction 10]. The 6-position of N-acetylgalactosamine is sulfated by Chst3 and Chst7 on either chondroitin or dermatan [reaction 9]. The GlcA residues of chondroitin and the IdoA residues of dermatan are 2-sulfated by Ust [Reaction 8]. The abundance of the disaccharide structures enclosed in dotted lines were determined and the corresponding data is shown in Table 1. (C) Transcript Analysis. Transcript levels for enzymes involved in chain modification corresponding to the reactions in (A) and (B) are shown. Relative transcript abundance for mESC (gray bars) and EB (red bars) and ExE (black bars) are plotted on a log scale for each gene assayed. See legend of Figure 2 for details.

the sonic hedgehog (SHH) signaling pathway, which is critically involved in embryonic development.[53] Versican also avidly binds HA,[54] suggesting coordinate regulation between HA biosynthesis and the expression of HA binding proteins. In the small leucine rich proteoglycan (SLRP) family, all the mRNA levels examined, i.e., decorin, biglycan, asporin, and epiphycan[55] showed substantial (>10-fold) differences between mESCs and EBs and ExE. Decorin and biglycan transcript levels were enhanced in both EBs and ExE. Decorin is localized in the ECM of collagen rich tissues and biglycan appears to have regulatory functions in the pericellular environment.[55] Asporin transcripts only increased in ExE and epiphycan transcripts only decreased in ExE. In the syndecan family of HS proteoglycans, only syndecan 3 showed a pronounced increase in transcript abundance in ExE. Syndecan 3 plays a major role in the regulation of energy balance[56] and in muscle fiber formation.[57] In the glypican family, glypican 3 and 6 showed large increases of transcripts in both EBs and ExE, whereas glypican 5 mRNA only increased in differentiation to EBs. Glypicans play a critical role in developmental morphogenesis[58,59] but prior studies have only examined glypicans role in the later stages of development.[60] Glypican 3 is expressed in embryogenesis[61] and directly affects insulin growth factor (IGF) signaling,[58] and glypican 5 and 6 are co-localized on human chromosome 13 and mouse chromosome 14.[62] Finally, thrombomodulin and collagen XVIII showed an increase in transcript levels in both EBs and ExE, whereas RPTP beta/phosphacan showed a decrease in transcript abundance in ExE and tenascin-C showed an increase in transcript levels in ExE. Thrombomodulin, critical in maintaining blood homeostasis, is expressed early in embryogenesis, prior to vascularization,[63] and appears to regulate apoptotic cell death in embryonic trophoblasts. Collagen XVIII is localized in the *sublamina densa* of the basement membrane and contributes to the anchoring of the basement membrane to the underlying structures.[64] A C-terminal domain fragment of collagen XVIII is endostatin, which is a prominent inhibitor of angiogenesis. Although both asporin and tenascin-C core proteins are not known to contain attached GAG chains in tissues previously studied,[65,66] it is possible that these core proteins may contain GAG chains in early development. It is also important to note that asporin and tenascin-C, as well as any of the other core proteins studied at the transcriptional level (Table 3), may not be post-translationally modified with GAG chains. Finally, it is interesting that the core proteins found to be transcriptionally up-regulated in mESC differentiation are commonly associated with cartilage, a tissue rich in ECM and not containing a basement membrane. This may correlate well with the loose, hydrated matrix associated with embryonic development.

The enzymes involved in the synthesis of the linkage region are believed to be a factor in directing GAG biosynthesis (Figure 6A). The initiation enzymes β-GalNAc transferase (Extl2 and Ext13) and α-GlcNAc transferase (GalNAct2) result in subsequent linkage region primer extension, directing either HS or CS/DS biosynthesis, respectively.[67] The differentiation of mESCs to EBs and ExE results in a slight decrease of α-GlcNAct2 transcripts and a slight increase in Ext12 transcripts in ExE and Extl3 in both EBs and ExE, consistent with a slightly greater increase in HS content over CS/DS content in EBs and ExE, compared to mESCs.

The chain extension enzymes for HS show only slight differences in transcript levels for mESCs and EBs. The Chys3 chain extension enzyme for CS/DS shows a pronounced transcript increase on differentiation, offering an explanation for the enhanced synthesis of CS/DS. The EXT gene family has been shown to be essential for HS biosynthesis and embryonic development in *Caenorhabditis elegans*,[68] and depleted expression of chondroitin synthases in *C. elegans* results in cytokinesis defects in early embryogenesis,[69] demonstrating the critical importance of these biosynthetic enzymes.

The mRNA for GAG chain modifying enzymes in CS/DS[70−72] all show subtle differences with the exception of both the GlcA 2-*O*ST (Ust) and GlcNAc 4,6-*O*ST, (GalNAc 4S6ST), which show over a 10-fold enhancement in EB and ExE cells. This is consistent with the observation of large increases in the amounts of 4S6S(S_E)sequence and small increases in 2S4S(S_B) and 2S6S(S_D) sequences (Table 1). The →4)-β-D-GlcA (1→3)-β-D-GalNAc4S6S (1→ (S_E) sequence is involved in critical receptor binding functions[73] and is also believed to terminate CS-A chains.[74]

The GAG chain modifying enzymes in HS biosynthesis are a much more complex story because of the multiple isoforms of the 6-*O*ST and 3-*O*ST enzymes involved late in the biosynthetic pathway.[71,75] These can afford the enormous structural diversity responsible for the interaction of HS with many different proteins.[75−77] In the early modification steps, transcript abundance for NDST-1 and NDST-2 show slight enhancement with differentiation and NDST-3 and NDST-4 transcripts were only detectable in EB cells. In the adult mouse, NDST-1 and NDST-2 show broad overlapping tissue distribution, whereas NDST-3 and NDST-4 are more restricted.[78,79] NDST-1 knockout mice die either before birth or soon after birth. In contrast, NDST-2 knockout mice have defective connective tissue mast cells, suggesting the importance of NDST-2 in the synthesis of the highly sulfated HS GAG, heparin, carried on the serglycin core protein. NDST-3 and NDST-4 are expressed primarily during embryonic development,[78,80,81] and the current study shows their transcripts increase in ExE cells as well. The 2-*O*ST (HS2st1) and C_5Epi (Glce), which typically act in concert to synthesize IdoA2S residues most commonly found in heparin, show similar expression levels in mESCs, EBs, and ExE, suggesting no alteration of the HS/heparin ratio on differentiation. A 2-*O*ST knockout in mice is neonatal lethal resulting in renal dysgenesis.[82] The Hs6st1 transcript levels remained unchanged. A 6-*O*ST-1 mutant was defective in FGF signaling.[83] Both Hs6st2 and HS6st3 transcript levels increased on differentiation, but the 6-*O*ST-2 and 6-*O*ST-3 isoforms have broad tissue distribution in adult mammals, and their sub-specificity is presently not well understood.[71] The 3-*O*ST isoforms show differential expression in patterns and intriguing sub-specificities.[71] Isoforms for 3-*O*ST (Hs3st1, Hs3st2, and Hs3st3a1) show transcript increases in EB and ExE cells. These enzymes are found in adult mouse kidney/brain (broad), brain and heart/placenta (broad) and act on →4)-β-D-GlcA (1→4)-α-D-GlcNS ± 6S(1→, →4)-β-D-HexA (1→4)-α-D-GlcNS(1→ and →4)-α-L-IdoA2S(1→4)-α-D-GlcN ± 6S(1→ sequences, respectively. A 3-*O*ST-1 knock out mouse mutant shows a subtle but complicated phenotype.[84] 3-*O*ST isoform-5 and isoform-6, with expression levels remaining unchanged from mESCs to EBs, or ExE, are found in the brain and brain/spinal cord and act on unknown or →4)-β-D-HexA ± 2S (1→4)-α-D-GlcNS ± 6S (1→ sequences, respectively. 3-*O*ST isoform-3b1, with unaltered transcript levels in differentiation, is found in the liver/placenta (broad distribution) of the adult mouse and acts on →4)-α-L-IdoA2S (1→4)-α-D-GlcN ± 6S (1→ sequences. The 3-*O*ST family of isoforms offers the greatest potential insight into subtle

changes in HS structure important to cell growth and cell differentiation.

In conclusion, the current study demonstrates an initial examination of the glycomics of mESC differentiation as it applies to GAG biosynthesis. These results provide the basis for devising and testing hypotheses that are focused on understanding specific steps in the biosynthesis of particular GAG biosynthetic products that we have shown to change with differentiation. Two specific examples illustrate the value of transcript levels of biosynthetic enzymes in predicting glycome composition and structure. The increased transcript expression levels of Has1 and Has2 parallel the 13- to 24-fold increase in HA observed on stem cell differentiation and the increased transcript levels GalNAc4S6ST correlates with the enhanced levels of 4S6S (S_E) and 2S4S (S_B) in both CS and DS. The confirmation of the importance of differential transcription levels for the 3-*O*-ST isoforms awaits the development of reliable analytical methods for determining products containing these structures.

Conclusions

A glycomics approach was successfully used to examine GAG content, composition and the level of transcripts encoding for GAG biosynthetic enzymes as murine embryonic stem cells (mESCs) differentiate to embryoid bodies (EBs) and to extraembryonic endodermal cells (ExE). The results obtained lead to better understand the role of GAGs in stem cell differentiation. Future studies will also examine the changes in expression levels of GAG-binding proteins that occur upon differentiation of mESCs to EBs and ExE in an effort to define the function of specific GAG structures on differentiation and cell growth during embryogenesis.

Acknowledgment. This research was supported by NIH grants HL62244, HL52622, GM38060 (to R.J.L.), and RR018502 (to K.W.M., S.D., and J.M.P.).

Supporting Information Available: Supplementary Table 1. This information is available free of charge via the Internet at http://pubs.acs.org.

References

(1) Linhardt, R. J.; Toida, T. Role of glycosaminoglycans in cellular communication. *Acc. Chem. Res.* **2004**, *37*, 431−438.
(2) Gama, C. I.; Hsieh-Wilson, L. C. Chemical approaches to deciphering the glycosaminoglycan code. *Curr. Opin. Chem. Biol.* **2005**, *9*, 609−619.
(3) Raman, R.; Sasisekharan, V.; Sasisekharan, R. Structural insights into biological roles of protein-glycosaminoglycan interactions. *Chem. Biol.* **2005**, *12*, 267−277.
(4) Habuchi, O.; Moroi, R.; Ohtake, S. Enzymatic synthesis of chondroitin sulfate E by N-acetylgalactosamine 4-sulfate 6-O-sulfotransferase purified from squid cartilage. *Anal. Biochem.* **2002**, *310*, 129−136.
(5) Hacker, U.; Nybakken, K.; Perrimon, N. Heparan sulphate proteoglycans: the sweet side of development. *Nat. Rev. Mol. Cell Biol.* **2005**, *6*, 530−541.
(6) Lin, X. Functions of heparan sulfate proteoglycans in cell signaling during development. *Development (Cambridge, U. K.)* **2004**, *131*, 6009−6021.
(7) Thisse, B.; Thisse, C. Functions and regulations of fibroblast growth factor signaling during embryonic development. *Dev. Biol.* **2005**, *287*, 390−402.
(8) Shriver, Z.; Liu, D.; Sasisekharan, R. Emerging views of heparan sulfate glycosaminoglycan structure/activity relationships modulating dynamic biological functions. *Trends Cardiovasc. Med.* **2002**, *12*, 71−77.
(9) Raman, R.; Raguram, S.; Venkataraman, G.; Paulson, J. C.; Sasisekharan, R. Glycomics: an integrated systems approach to structure-function relationships of glycans. *Nat. Methods* **2005**, *2*, 817−824.
(10) Warda, M.; Toida, T.; Zhang, F.; San, P.; Munoz, E.; Linhardt, R. J. Isolation and characterization of heparan sulfate from various murine tissues. *Glycoconjate J.* **2006**, *23*, 553−561.
(11) Ledin, J.; Swattz, W.; Li, J.-P.; Gotte, M.; Selleck, S.; Kjellén, L.; Spillmann, D. Heparan sulfate structure in mice with genetically modified heparan sulfate production. *J. Biol. Chem.* **2004**, *279*, 42732−42741.
(12) Evans, M. J.; Kaufman, M. H. Establishment in culture of pluripotential cells from mouse embryos. *Nature* **1981**, *292*, 154−156.
(13) Martin, G. R. Isolation of a pluripotent cell line from early mouse embryos cultured in medium conditioned by teratocarcinoma stem cells. *Proc. Natl. Acad. Sci. U.S.A.* **1981**, *78*, 7634−7636.
(14) Brook, F. A.; Gardner, R. L. The origin and efficient derivation of embryonic stem cells in the mouse. *Proc. Natl. Acad. Sci. U.S.A.* **1997**, *94*, 5709−5712.
(15) Bradley, A.; Evans, M.; Kaufman, M.; Robertson, E. Formation of germ-line chimaeras from embryo-derived teratocarcinoma cell lines. *Nature* **1984**, *309*, 255−256.
(16) Pederson, R. A. Studies of in vitro differentiation with embryonic stem cells. *Reprod., Fertil. Dev.* **1994**, *6*, 543−552.
(17) Smith, A.; Heath, J. K.; Donaldson, D. D.; Wong, G. G.; Moreau, J.; Stahl, M.; Rogers, D. Inhibition of pluripotential embryonic stem cell differentiation by purified polypeptides. *Nature* **1988**, *336*, 688−690.
(18) Williams, R. L.; Hilton, D. J.; Pease, S.; Wilson, T. A.; Stewart, C. L.; Gearing, D. P.; Wagner, E. F.; Metcalf, D.; Nicola, N. A.; Gough, N. Myeloid leukaemia inhibitory factor maintains the developmental potential of embryonic stem cells. *Nature* **1988**, *336*, 684−687.
(19) Nichols, J.; Evans, E. P.; Smith, A. G. Establishment of germ-line-competent embryonic stem (ES) cells using differentiation inhibiting activity. *Development (Cambridge, U. K.)* **1990**, *110*, 1341−1348.
(20) Pease, S.; Braghetta, P.; Gearing, D.; Grail, D.; Williams, L. Isolation of embryonic stem (ES) cells in media supplemented with recombinant leukemia inhibitory factor. *Dev. Biol.* **1990**, *141*, 344−352.
(21) Robertson, E.; Bradley, A.; Kuehn, M.; Evans, M. Germ-line transmission of genesintroduced into cultured pluripotential cells by retroviral vector. *Nature* **1986**, *323*, 445−448.
(22) Thomas, K. R.; Capecchi, M. R. Site-directed mutagenesis by gene targeting in mouse embryo-derived stem cells. *Cell* **1987**, *51*, 503−512.
(23) Beddington, R. S. P.; Robertson, E. J. An assessment of the developmental potential of embryonic stem cells in the midgestation mouse embryo. *Development (Cambridge, U. K.)* **1989**, *105*, 733−737.
(24) Doetschman, T. C.; Eistetter, H.; Schmidt, K. M.; Kemler, R. The in vitro development of blastocyst-derived embryonic stem cell lines: formation of visceral yolk sac, blood islands and myocardium. *J. Embryol. Exp. Morph.* **1985**, *87*, 27−45.
(25) Smith, A. G. Culture and differentiation of embryonic stem cells. *J. Tissue Cult. Methods* **1991**, *13*, 89−94.
(26) Hadjantonakis, A. K.; Gertsenstein, M.; Ikawa, M.; Okabe M.; Nagy, A. Generating green fluorescent mice by germline transmission of green fluorescent ES cells. *Mech. Dev.* **1998**, *76*, 79−90.
(27) Rathjen, J.; Lake, J.-A.; Bettess, M. D.; Washington, J. M.; Chapman, G.; Rathjen, P. D. Formation of a primitive ectoderm like cell population, EPL cells, from ES cells in response to biologically derived factors. *J. Cell Sci.* **1999**, *112*, 601−612.
(28) Lake, J.; Rathjen, J;, Remiszewski, J.; Rathjen, P. D. Reversible programming of pluripotent cell differentiation. *J. Cell Sci.* **2000**, *113*, 555−566.
(29) Capo-chichi, C.; Rula, M. E.; Smedberg, J. L.; Vanderveer, L.; Parmacek, M. S.; Morrisey, E. E.; Godwin, A. K.; Xu, X. X. Perception of differentiation cues by GATA factors in primitive endoderm lineage determination of mouse embryonic stem cells. *Dev. Biol.* **2005**, *286*, 574−586.
(30) Toyoda, H.; Kinoshita-Toyoda, A.; Selleck, S. B. Structural analysis of glycosaminoglycans in Drosophila and Caenorhabditis elegans and demonstration that tout-velu, a Drosophila gene related to EXT tumor suppressors, affects heparan sulfate *in vivo*. *J. Biol. Chem.* **2000**, *275*, 2269−2275.

(31) Mada, A.; Toyoda, H.; Imanari, T. Utility of a carbon column for high performance liquid chromatographic separation of unsaturated disaccharides produced from glycosaminoglycans. *Anal. Sci.* **1992**, *8*, 793−797.
(32) Pfaffl, M. W. A new mathematical model for relative quantification in real-time RT-PCR. *Nucleic Acids Res.* **2001**, *29*, 2002−2007.
(33) Ramakers, C.; Ruijter, J. M.; Deprez, R. H.; Moorman, A. F. Assumption-free analysis of quantitative real-time polymerase chain reaction (PCR) data. *Neurosci. Lett.* **2003**, *339*, 62−66.
(34) Kamiyama, S.; Suda, T.; Ueda, R.; Suzuki, M.; Okubo, R.; Kikuchi, N.; Chiba, Y.; Gota, S.; Toyoda, H.; Saigo, K.; Watanabe, M.; Narimatsu, H.; Jigami, Y.; Nishihara, S. Molecular cloning and identification of 3′-phosphoadenosine 5′-phosphosulfate transporter. *J. Biol. Chem.* **2003**, *278*, 25958−25963.
(35) Toole, B. P. Hyaluronan in morphogenesis. *Semin. Cell Dev. Biol.* **2001**, *12*, 79−87.
(36) Itano, N.; Sawai, T.; Yoshida, M.; Lenas, P.; Yamada, Y.; Imagawa, M.; Shinomura, T.; Hamaguchi, M.; Yoshida, Y.; Ohnuki, Y.; Miyauchi, S.; Spicer, A. P.; McDonald, J. A.; Kimata, K. Three isoforms of mammalian hyaluronan synthases have distinct enzymatic properties. *J. Biol. Chem.* **1999**, *274*, 25085−25092.
(37) Itano, N.; Kimata, K. Mammalian hyaluronan synthases. *Life* **2002**, *54*, 195−199.
(38) Brown, J. J.; Papaioannou, V. E. Ontogeny of hyaluronan secretion during early mouse development. *Development (Cambridge, U. K.)* **1993**, *117*, 483−492.
(39) Kosaki, R.; Watanabe, K.; Yamaguchi, Y. Overproduction of hyaluronan by expression of the hyaluronan synthase Has2 enhances anchorage-independent growth and tumorigenicity. *Cancer Res.* **1999**, *59*, 1141−1145.
(40) Fraser, J. R.; Laurent, T. C.; Pertoft, H.; Baxter, E. Plasma clearance, tissue distribution and metabolism of hyaluronic acid injected intravenously in the rabbit. *Biochem. J.* **1981**, *200*, 415−424.
(41) Stern, R. Devising a pathway for hyaluronan catabolism: are we there yet? *Glycobiology* **2003**, *13*, 105R−115R.
(42) Triggs-Raine, B.; Salo, T. J.; Zhang, H.; Wicklow, B. A.; Natowicz, M. R. Mutations in HYAL1, a member of a tandemly distributed multigene family encoding disparate hyaluronidase activities, cause a newly described lysosomal disorder, mucopolysaccharidosis IX. *Proc. Natl. Acad. Sci. U.S.A.* **1999**, *96*, 6296−6300.
(43) Flannery, C. R.; Little, C. B.; Hughes, C. E.; Caterson, B. Expression and activity of articular cartilage hyaluronidases. *Biochem. Biophys. Res. Commun.* **1998**, *251*, 824−829.
(44) Nicoll, S. B;, Barak, O.; Csoka, A. B.; Bhatnagar, R. S.; Stern, R. Hyaluronidases and CD44 undergo differential modulation during chondrogenesis. *Biochem. Biophys. Res. Commun.* **2002**, *292*, 819−825.
(45) Baba, D.; Kashinwabara, S.; Honda, A.; Yamagata, K.; Wu, Q.; Ikawa, M.; Okabe, M.; Baba, T. Mouse sperm lacking cell surface hyaluronidase PH-20 can pass through the layer of cumulus cells and fertilize the egg. *J. Biol. Chem.* **2002**, *227*, 30310−30314.
(46) Myles, D. G.; Primakoff, P. Why did the sperm cross the cumulus? To get to the oocyte. Functions of the sperm surface proteins PH-20 and fertilin in arriving at, and fusing with, the egg. *Biol. Reprod.* **1997**, *56*, 320−327.
(47) Csoka, A. B.; Scherer, S. W.; Stern, R. Expression analysis of six paralogous human hyaluronidase genes clustered on chromosomes 3p21 and 7q31. *Genomics* **1999**, *60*, 356−361.
(48) Beech, D. J.; Madan, A. K.; Deng, N. Expression of PH-20 in normal and neoplastic breast tissue. *J. Surg. Res.* **2002**, *103*, 203−207.
(49) Schick, B. P.; Ho, H. C.; Brodbeck, K. C.; Wrigley, C. W.; Klimas, J. Serglycin proteoglycan expression and synthesis in embryonic stem cells. *Biochim. Biophys. Acta* **2003**, *1593*, 259−267.
(50) Sutherland, A. E.; Sanderson, R. D.; Mayes, M.; Seibert, M.; Calarco, P. G.; Bernfield, M.; Damsky, C.; H. Expression of syndecan, a putative low affinity fibroblast growth factor receptor, in the early mouse embryo. *Development (Cambridge, U. K.)* **1991**, *113*, 339−351.
(51) French, M. M.; Smith, S. E.; Akanbi, K.; Sanford, T.; Hecht, J.; Farach-Carson, M. C.; Carson, D. D. Expression of the heparan sulfate proteoglycan, perlecan, during mouse embryogenesis and perlecan chondrogenic activity in vitro. *J. Cell Biol.* **1999**, *145*, 1103−1115.
(52) Capo-Chichi, C. D.; Rula, M. E.; Smedberg, J. L.; Vanderveer, L.; Parmacek, M. S.; Morrisey, E. E.; Godwin, A. K.; Xu, X. X. Perception of differentiation cues by GATA factors in primitive endoderm lineage determination of mouse embryonic stem cells. *Dev. Biol.* **2005**, *286*, 574−586.
(53) Rahmani, M.; Wong, B. W.; Ang, L.; Cheung, C. C.; Carthy, J. M.; Walinski, H.; McManus, B. M. Versican: signaling to transcriptional control pathways. *Can. J. Physiol. Pharmacol.* **2006**, *84*, 77−92.
(54) Wight, T. N. Versican: a versatile extracellular matrix proteoglycan in cell biology. *Curr. Opin. Cell. Biol.* **2002**, *14*, 617−623.
(55) Young, M. F.; Bi, Y.; Ameye, L.; Chen, X. D. Biglycan knockout mice: new models for musculoskeletal diseases. *Glycoconj. J.* **2002**, *19*, 257−262.
(56) Reizes, O.; Clegg, D. J.; Strader, A. D.; Benoit, S. C. A role for syndecan-3 in the melanocortin regulation of energy balance. *Peptides* **2006**, *27*, 274−280.
(57) Casar, J. C.; Cabello-Verrugio, C.; Olguin, H.; Aldunate, R.; Inestrosa, N. C.; Brandan, E. Heparan sulfate proteoglycans are increased during skeletal muscle regeneration: requirement of syndecan-3 for successful fiber formation. *J. Cell Sci.* **2004**, *117*, 73−84.
(58) Filmus, J.; Selleck, S. B. Glypicans: proteoglycans with a surprise. *J. Clin. Invest.* **2001**, *108*, 497−501.
(59) Hufnagel, L.; Kreuger, J.; Cohen, S. M.; Shraiman, B. I. On the role of glypicans in the process of morphogen gradient formation. *Dev. Biol.* **2006**, *300*, 512−522.
(60) Song, H. H.; Filmus, J. The role of glypicans in mammalian development. *Biochem. Biophys. Acta* **2002**, *1573*, 241−246.
(61) Grozdanov, P. N.; Yovchev, M. I.; Dabeva, M. D. The oncofetal protein glypican-3 is a novel marker of hepatic progenitor/oval cells. *Lab. Invest.* **2006**, *86*, 1272−1284.
(62) Paine-Saunders, S.; Viviano, B. L.; Saunders, S. GPC6, a novel member of the glypican gene family, encodes a product structurally related to GPC4 and is colocalized with GPC5 on human chromosome 13. *Genomics* **1999**, *57*, 455−458.
(63) Weiler, H.; Isermann, B. H. Thrombomodulin. *J. Thromb. Haemost.* **2003**, *1*, 1515−*1524.*
(64) Marneros, A. G.; Olsen, B. R. Physiological role of collagen XVIII and endostatin. *FASEB J.* **2005**, *19*, 716−728.
(65) Lorenzo, P.; Aspberg, A.; Onnerfjord, P.; Bayliss, M. T.; Neame, P. J.; Heinegard, D. Identification and characterization of asporin. a novel member of the leucine-rich repeat protein family closely related to decorin and biglycan. *J. Biol. Chem.* **2001**, *276*, 12201−12211.
(66) Chiquet-Ehrismann, R. Tenascins. *Int. J. Biochem. Cell Biol.* **2004**, *36*, 986−990.
(67) Sugahara, K.; Kitagawa, H. Recent advances in the study of the biosynthesis and functions of sulfated glycosaminoglycans. *Curr. Opin. Struct. Biol.* **2000**, *10*, 518−527.
(68) Morio, H.; Honda, Y.; Toyoda, H.; Nakajima, M.; Kurosawa, H.; Shirasawa, T. EXT gene family member rib-2 is essential for embryonic development and heparan sulfate biosynthesis in Caenorhabditis elegans. *Biochem. Biophys. Res. Comm.* **2003** *301*, 317−323.
(69) Mizuguchi, S.; Uyama, T.; Kitagawa, H.; Nomura, K. H.; Dejima, K.; Gengyo-Ando, K.; Mitani, S.; Sugahara, K.; Nomura, K. Chondroitin proteoglycans are involved in cell division of Caenorhabditis elegans. *Nature* **2003**, *423*, 443−448.
(70) Grunwell, J.; Bertozzi, C. R. Carbohydrate sulfotransferases of the GalNAc/Gal/GlcNAc6ST family. *Biochemistry* **2002**, *41*, 13117−13126.
(71) Kusche-Gullberg, M.; Kjellén, L. Sulfotransferases in glycosaminoglycan biosynthesis. *Curr. Opin. Struct. Biol.* **2003**, *13*, 605−611.
(72) Bergefall, K.; Trybala, E.; Johansson, M.; Uyama, T.; Naito, S.; Yamada, S.; Kitagawa, H.; Sugahara, K.; Bergstrom, T. Chondroitin sulfate characterized by the E-disaccharide unit is a potent inhibitor of herpes simplex virus infectivity and provides the virus binding sites on gro2C cells. *J. Biol. Chem.* **2005**, *280*, 32193−32199.
(73) Nandini, C. D.; Sugahara, K. Role of the sulfation pattern of chondroitin sulfate in its biological activities and in the binding of growth factors. *Adv. Pharmacol.* **2006**, *53*, 253−279.
(74) Ohtake, S.; Kimata, K.; Habuchi, O. A unique nonreducing terminal modification of chondroitin sulfate by N-acetylgalactosamine 4-sulfate 6-O-sulfotransferase. *J. Bio. Chem.* **2003**, *278*, 38443−38452.
(75) Esko, J. D.; Selleck, S. B.; Order out of chaos: assembly of ligand binding sites in heparan sulfate. *Annu. Rev. Biochem.* **2002**, *71*, 435−471.
(76) Rabenstein, D. L. Heparin and heparan sulfate: structure and function. *Nat. Prod. Rep.* **2002**, *19*, 312−331.
(77) Linhardt, R. J.; Capila, I. Heparin-protein interactions. *Angew. Chem., Int. Ed.* **2002**, *41*, 390−412.

(78) Grobe, K.; Ledin, J.; Ringvall, M.; Holmborn, K.; Forsberg, E.; Esko, J.; Kjellén, L.; Heparan sulfate and development: differential roles of the N-acetylglucosamine N-deacetylase/N-sulfotransferase isozymes. *Biochem. Biophys.* **2002**, *1573*, 209−215.
(79) Kjellén, L. Glucosaminyl N-deacetylase/N-sulphotransferases in heparan sulphate biosynthesis and biology. *Biochem. Soc.* **2003**, *31*, 340−342.
(80) Aikawa, J.; Grobe, K.; Tsujimoto, M.; Esko, J. D. Multiple isozymes of heparan sulfate/heparin GlcNAc N-deacetylase/GlcN N-sulfotransferase. Structure and activity of the fourth member, NDST4. *J. Biol. Chem.* **2001**, *276*, 5876−5882.
(81) Aikawa, J.; Esko, J. D. Molecular cloning and expression of a third member of the heparan sulfate/heparin GlcNAc N-deacetylase/N-sulfotransferase family. *J. Biol. Chem.* **1999**, *274*, 2690−2695.
(82) Bullock, S. L.; Fletcher, J. M.; Beddington, R. S. P.; Wilson, V. A. Renal agenesis in mice homozygous for a gene trap mutation in the gene encoding heparan sulfate 2-sulfotransferas. *Genes Dev.* **1998** *12*, 1894−1906.
(83) Kamimura, K.; Fujise, M.; Villa, F.; Izumi, S.; Habuchi, H.; Kimata, K.; Nakato, H. Drosophila heparan sulfate 6-O-sulfotransferase (dHS6ST) gene. Structure, expression, and function in the formation of the tracheal system. *J. Biol. Chem.* **2001**, *276*, 17014−17021.
(84) de Agostini, A. L.; Lau, H. K.; Leone, C.; Youssoufian, H.; Rosenberg, R. D. Cell mutants defective in synthesizing a heparan sulfate proteoglycan with regions of defined monosaccharide sequence. *Proc. Natl. Acad. Sci. U.S.A.* **1990**, *87*, 9784−9788.
(85) Silbert, J. E.; Sugumaran, G. A starting place for the road to function. *Glycoconj. J.* **2002**, *19*, 227−237.
(86) Miller, J.; Hatcht, J. A.; Simonist, S.; Cullent, S. E. Identification of the glycosaminoglycan-attachment site of mouse invariant-chain proteoglycan core protein by site-directed mutagenesis. *Proc. Natl. Acad. Sci. U.S.A.* **1988**, *85*, 1359−1363.
(87) Lorenzo, P.; Aspberg, A.; O'nnerfjord, P.; Bayliss, M. T.; Neame, P. J.; Heinegård, D. Identification and characterization of asporin. A novel member of the leucine-rich repeat protein family closely related to decorin and biglycan. *J. Biol. Chem.* **2001**, *276*, 12201−12211.
(88) Groffen, A. J. A.; Buskens, C. A. F.; Van, Kuppevelt, T. H.; Veerkamp, J. H.; Monnen, L. A. H.; Van Den Heuvel, L. P. W. J. Primary structure and high expression of human agrin in basement membranes of adult lung and kidney. *Eur. J. Biochem.* **1998**, *254*, 123−128.
(89) Elamaa, H.; Snellman, A.; Rehn, M.; Autio-Harmainen, H.; Pihlajaniemi, T. Characterization of the human type XVIII collagen gene and proteolytic processing and tissue location of the variant containing a frizzled motif. *Matrix Biol.* **2003**, *22*, 427−442.

PR070446F